

Analytical Solution of Transient Heat Conduction through a Hollow Cylindrical Thermal Insulation Material of a Temperature Dependant Thermal Conductivity

Dr. Mishaal Abdulameer Abdulkareem

Lecturer, Mechanical Engineering Department

College of Engineering, Al-Mustansiriyah University, Baghdad, Iraq

dr.mishal04@gmail.com

ABSTRACT

The one-dimensional, cylindrical coordinate, non-linear partial differential equation of transient heat conduction through a hollow cylindrical thermal insulation material of a thermal conductivity temperature dependent property proposed by an available empirical function is solved analytically using Kirchhoff's transformation. It is assumed that this insulating material is initially at a uniform temperature. Then, it is suddenly subjected at its inner radius with a step change in temperature. Four thermal insulation materials were selected. An identical analytical solution was achieved when comparing the results of temperature distribution with available analytical solution for the same four case studies that assume a constant thermal conductivity. It is found that the characteristics of the thermal insulation material and the pressure value between its particles have a major effect on the rate of heat transfer and temperature profile.

KEYWORDS: Nonlinear differential equation, analytical solution, thermal conductivity, transient, Kirchhoff's transformation.

حل تحليلي لتوصيل الحرارة المتغير مع الزمن خلال مادة أسطوانية مجوفة عازلة للحرارة ذات توصيل حراري متغير مع درجة الحرارة

د. مشعل عبد الأمير عبد الكريم
مدرس في قسم الهندسة الميكانيكية
الجامعة المستنصرية / كلية الهندسة

الخلاصة

تم حل المعادلة التفاضلية الغير خطية الأحادية البعد ذو الإحداثيات الأسطوانية لانتقال الحرارة المتغير مع الزمن خلال مادة أسطوانية مجوفة عازلة للحرارة ذات خاصية توصيل حراري متغير مع درجة الحرارة مأخوذة من معادلة مختبريه متوفرة باستخدام تحويل كرشوف. تم افتراض أن هذه المادة العازلة كانت في البداية بدرجة حرارة منتظمة وثابتة. ثم تعرضت إلى تغير مفاجئ في درجة الحرارة وبقيمة ثابتة عند نصف قطرها الداخلي. تم اختيار أربعة مواد عازلة مختلفة. تم التوصل إلى حل تحليلي مطابق عند المقارنة مع نتائج الحل التحليلي لتوزيع درجات الحرارة للحالات الأربعة بافتراض إن المادة العازلة للحرارة ذو خاصية توصيل حراري ثابتة ولا تتغير مع درجة الحرارة. تم استنتاج إن خواص المادة العازلة للحرارة وقيمة الضغط بين جزيئاتها له تأثير مباشر على مقدار كمية الحرارة المنتقلة وتوزيع درجات الحرارة.

الكلمات الرئيسية: معادلة تفاضلية غير خطية ، حل تحليلي ، توصيل حراري ، متغير مع الزمن ، تحويل كرشوف.

1. INTRODUCTION

The performance of air separation plants, storage tanks, transfer lines and transport vessels for cryogenic liquids and liquefied hydrocarbons depends majorly on the characteristics of its thermal insulating materials. Most of these thermal insulations operate under atmospheric or medium vacuum pressure, and it use either Perlite (a loose granulated material of volcanic glass origin heated at 850-900 C° to vaporize the high water content that is trapped in its structure and allowing its volume to be porous and expanded up to 7–16 times its original volume), or mineral fibers in the form of shells or mats (Verschoor and Greebler, 1952), (Kropschot and Burges, 1962) and (Kaganer, 1969). For specific applications, when only a small space is available for thermal insulation, a system of multilayered foils is used in a high vacuum. It is preferred in the field of transfer lines of liquid hydrogen and liquid helium as well as components in the space technology and in the field of physical basic experimental research (Hoffman, 2006). A common property of all cryogenic thermal insulating materials is that it operates under high temperature deference between atmospheric air and cryogenic fluid temperatures. Therefore, filling it inside a vacuumed leak tight annular space separating the atmosphere from cryogenic fluid vessels is necessary to avoid the drop in its efficiency due to the penetration and freeze of water vapor and carbon dioxide.

The sudden filling of an empty cryogenic liquid storage tank initially at atmospheric temperature with a cryogenic liquid at its saturation temperature will initiate a sudden high temperature difference between the terminals of the annular space containing the thermal insulating material. This high temperature difference is behind the dependence of thermal conductivity of the thermal insulation material on its temperature. In addition, it will initiate a potential for the evaporation of cryogenic liquid due to the transient heat transfer inside the cryogenic liquid storage tank. This energy loss is of a great economic interest especially when the size of cryogenic liquid storage tank is relatively big.

(Zivkovic et al, 2010) have used the PAK-T software package, which is based on the finite element method using the Galerkin approach to solve the non-linear transient two-dimensional heat conduction through an insulation wall of tank for transportation of liquid aluminum. The objective was to optimize, under certain boundary conditions, the thickness of the insulation material which its thermal properties is a temperature dependent.

(Singh, Jain and Rizwan-Uddin, 2008) presented an analytical double-series solution for transient heat conduction in polar coordinates (2-D cylindrical) for multi-layer domain in the radial direction with spatially non-uniform but time-independent volumetric heat sources. Inhomogeneous boundary conditions of the third kind are applied in the direction perpendicular to the layers. Only homogeneous boundary conditions of the first or second kind are applicable on $\theta = \text{constant}$ surfaces.

(Amiri, Kayhani and Norouzi, 2012) have investigated analytically the unsteady heat conduction in composite fiber winded cylindrical shape laminates. This solution is valid for the most generalized boundary conditions that combine the effects of conduction, convection and radiation both inside and outside the cylindrical composite laminates. The Laplace transformation has been used to change the problem domain from time into frequency. An appropriate Fourier transformation has been derived using the Sturm-Liouville theorem. Due to the difficulty of applying the inverse Laplace transformation, the Meromorphic function method is utilized to find the transient temperature distribution in laminate.

In this paper, the one-dimensional, cylindrical coordinate, non-linear partial differential equation of transient heat conduction through a hollow cylindrical thermal insulation material of a thermal conductivity temperature dependent property proposed by an available empirical function ($k = a + bT^c$), (Hoffman, 2006), is solved analytically using Kirchoff's transformation. This insulating material is



initially at a uniform temperature (T_i). Then, it is suddenly subjected at its internal radius ($r = R_1$) to a constant temperature (T_o), ($T_o < T_i$). Four thermal insulation materials were selected, (Hoffman, 2006), each of outside radius of (1m). The first is Perlite of thickness (800mm) with a characteristic mean particle diameter of ($d_m = 0.5mm$) and density of ($\rho = 64kg/m^3$) at ($10^5 Pa$) atmospheric pressure. The second is Perlite of thickness (600mm) with a characteristic mean particle diameter of ($d_m = 0.5mm$) and density of ($\rho = 50kg/m^3$) at a gas pressure ($\leq 0.1Pa$). The third is Microglass spheres of thickness (400mm) with a characteristic mean particle diameter of ($d_m = 0.1mm$) and density of ($\rho = 225kg/m^3$) at a gas pressure ($\leq 1Pa$). The fourth is micro fine Fiberglass mats of thickness (200mm) with a mean fiber diameter of ($d_m = 1.143\mu m$) and density of ($\rho = 240kg/m^3$) at a gas pressure ($\leq 1Pa$). To validate the results, the temperature distribution will be compared with an available analytical solution for the same four case studies that assume a constant thermal conductivity. A summary table will present the general analytical solution for the history of temperature profiles and heat transfer rates of any size and type of thermal insulation material that is subjected at ($r = R_1$) with a constant temperature (T_o), ($T_o < T_i$).

2. STATEMENT OF THE PROBLEM

Consider a cylindrical storage tank of liquefied cryogenic fluid is thermally insulated with a hollow cylindrical super insulating material of temperature dependent thermal conductivity proposed by an available empirical function ($k = a + bT^c$), and of inside radius (R_1) and outside radius (R_2). This insulating material is initially at a uniform temperature (T_i). Then, it is suddenly subjected at ($r = R_1$) with a constant

temperature (T_o), ($T_o < T_i$) as shown in **Fig. 1**. It is required to find the transient temperature distribution of the insulating material and the rate of heat transfer.

3. ANALYTICAL SOLUTION

To solve this problem, the following assumptions are considered:

1. The temperature is a function of (r, t) only, (Transient, One-dimensional solution), and no heat transfer in (θ and z) directions.
2. The temperature dependant thermal conductivity of the insulating material is proposed by an available empirical function ($k = a + bT^c$).
3. The mean specific heat capacity (C_m) and the density (ρ) of the insulating material are temperature independent properties.
4. The initial temperature of the insulating material is constant (T_i).
5. The insulating material is suddenly subjected at ($r = R_1$) with a constant temperature (T_o) and held at its initial temperature value (T_i) at its outside surface at ($r = R_2$).
6. No convection or radiation heat transfer at the boundaries.
7. No internal heat generation.

Since all of the thermal properties of the insulating material are temperature independent except the thermal conductivity, which is a temperature dependent property, and there is no heat generation and no convection or radiation heat transfer at the boundaries. Therefore, the cylindrical coordinates, one-dimensional, non-linear transient heat conduction partial differential equation, with its initial and Dirichlet boundary condition are given as follows:

$$\left. \begin{aligned} \rho C_m \frac{\partial T}{\partial t} &= \frac{1}{r} \frac{\partial}{\partial r} \left(r k(T) \frac{\partial T}{\partial r} \right) \\ T(r,0) &= T_i \\ T(R_1,t) &= T_o \\ T(R_2,t) &= T_i \end{aligned} \right\} \quad (1)$$

To linearize the non-linear partial differential equation in system (1), a corrected Kirchhoff's transformation, (Arpaci, 1966), in accordance to the zero lower limit of the absolute temperature scale, as shown in **Fig. 2**, is used as follows:

$$\psi = \int_0^{T^{**}} k(T) dT \quad (2)$$

Substituting eq. (2) into system (1) and rearranging yields;

$$\left. \begin{aligned} \rho C_m \frac{1}{k(T)} \frac{\partial \psi}{\partial t} &= \frac{1}{r} \frac{\partial}{\partial r} \left(r \frac{\partial \psi}{\partial r} \right) \\ \psi(r,0) &= \psi_i \\ \psi(R_1,t) &= \psi_o \\ \psi(R_2,t) &= \psi_i \end{aligned} \right\} \quad (3)$$

$$\psi_i = \int_0^{T_i} k(T) dT$$

$$\mu_i = \int_{T_i}^{T_o} k(T) dT$$

$$\psi_o = \psi_i + \mu_i$$

To homogenize system (3), assume;

$$\Omega = \psi - \psi_i \quad (4)$$

Substitute eq. (4) into system (3) and rearranging, yields;

$$\left. \begin{aligned} \rho C_m \frac{1}{k(T)} \frac{\partial \Omega}{\partial t} &= \frac{\partial^2 \Omega}{\partial r^2} + \frac{1}{r} \frac{\partial \Omega}{\partial r} \\ \Omega(r,0) &= 0 \\ \Omega(R_1,t) &= \mu_i \\ \Omega(R_2,t) &= 0 \end{aligned} \right\} \quad (5)$$

Assume:

$$\left. \begin{aligned} \theta &= \frac{\psi - \psi_o}{\psi_i - \psi_o} = \frac{\Omega - \mu_i}{-\mu_i} \\ \Omega &= -\mu_i \theta + \mu_i \end{aligned} \right\} \quad (6)$$

Substitute eq. (6) into system (5) and rearranging yields;

$$\left. \begin{aligned} \frac{1}{\alpha_m} \frac{\partial \theta}{\partial t} &= \frac{\partial^2 \theta}{\partial r^2} + \frac{1}{r} \frac{\partial \theta}{\partial r} \\ \theta(r,0) &= 1 \\ \theta(R_1,t) &= 0 \\ \theta(R_2,t) &= 1 \end{aligned} \right\} \quad (7)$$

$$\alpha_m = \frac{k_m}{\rho C_m}$$

$$k_m = \frac{\int_{T_i}^{T_o} k(T) dT}{T_o - T_i} = \frac{\mu_i}{T_o - T_i}$$

$$C_m = \frac{\int_{T_i}^{T_o} C(T) dT}{T_o - T_i}$$

To solve system (7), assume;

$$\theta(r,t) = \theta_1(r) + \theta_2(r,t) \quad (8)$$

$$\theta_1(r) = c_1 \ln(r) + c_2 \quad (9)$$

Substitute the boundary conditions of system (7) into eq. (9) and rearranging, yields;

$$\theta_1(r) = \frac{\ln(r/R_1)}{\ln(R_2/R_1)} \quad (10)$$

Assume;

$$\theta_2(r,t) = R(r)\tau(t) \quad (11)$$



Substituting eq. (11) into system (7) and using the method of separation of variables, then rearranging, yields;

$$R(r) = c_1 J_0(\lambda r) + c_2 Y_0(\lambda r) \tag{12}$$

$$\tau(t) = c_3 e^{-\lambda^2 \alpha_m t} \tag{13}$$

Substitute eq. (10), (12) and (13) into eq. (8), yields;

$$\theta(r, t) = \left[\frac{\ln(r/R_1)}{\ln(R_2/R_1)} \right] + [c_1 J_0(\lambda r) + c_2 Y_0(\lambda r)] c_3 e^{-\lambda^2 \alpha_m t} \tag{14}$$

To estimate the value of (λ) , substitute the boundary condition of system (7) into eq. (14) and rearranging yields;

$$c_2 = -c_1 \frac{J_0(\lambda R_2)}{Y_0(\lambda R_2)}$$

$$\frac{J_0(\lambda R_1)}{Y_0(\lambda R_1)} = \frac{J_0(\lambda R_2)}{Y_0(\lambda R_2)} \Rightarrow \frac{J_0(\lambda R_1)}{J_0(\lambda R_2)} = \frac{Y_0(\lambda R_1)}{Y_0(\lambda R_2)} = \sigma$$

$$J_0(\lambda_n R_1) Y_0(\lambda_n R_2) - J_0(\lambda_n R_2) Y_0(\lambda_n R_1) = 0 \tag{15}$$

The values of (λ_n) represent the roots of eq. (15), where $(n = 1, 2, 3, \dots, \infty)$. Assume:

$$U_0(\lambda_n r) = \frac{J_0(\lambda_n r) Y_0(\lambda_n R_2) - J_0(\lambda_n R_2) Y_0(\lambda_n r)}{J_0(\lambda_n R_2) Y_0(\lambda_n r)} \tag{16}$$

Substitute the initial condition of system (7) into eq. (14), and use eq. (16), then rearranging, yields;

$$f(r) = Y_0(\lambda_n R_2) \left[1 - \frac{\ln(r/R_1)}{\ln(R_2/R_1)} \right]$$

Hence;

$$f(r) = \sum_{n=1}^{\infty} c_n U_0(\lambda_n r) \quad , \quad \text{Where: } c_n = c_1 c_3$$

$$f(r) = c_1 U_0(\lambda_1 r) + c_2 U_0(\lambda_2 r) + c_3 U_0(\lambda_3 r) + \dots \tag{17}$$

$$= \sum_{n=1}^{\infty} c_n U_0(\lambda_n r)$$

Multiply eq. (17) by $[rU_0(\lambda_m r)]$ and integrate the result over the interval $[R_1, R_2]$ with the assumption that the integral of the infinite sum is equivalent to the sum of the integration (Arpaci, 1966), we have;

$$\int_{R_1}^{R_2} r f(r) U_0(\lambda_m r) dr = \sum_{n=1}^{\infty} c_n \int_{R_1}^{R_2} r U_0(\lambda_m r) U_0(\lambda_n r) dr \tag{18}$$

All the terms on the right hand side of eq. (18) equals zero, except when $(m = n)$, hence;

$$c_n = \frac{\int_{R_1}^{R_2} r f(r) U_0(\lambda_n r) dr}{\int_{R_1}^{R_2} r U_0^2(\lambda_n r) dr} \tag{19}$$

The denominator of eq. (19) is estimated as follows, (Carslaw and Jaeger, 1959);

$$\int_{R_1}^{R_2} r U_0^2(\lambda_n r) dr = \frac{2[J_0^2(\lambda_n R_1) - J_0^2(\lambda_n R_2)]}{\pi^2 \lambda_n^2 J_0^2(\lambda_n R_1)} \tag{20}$$

To estimate the nominator of eq. (19), the following are used, (Carslaw and Jaeger, 1959);

$$\int_{R_1}^{R_2} r U_0(\lambda_n r) dr = \frac{2[J_0(\lambda_n R_1) - J_0(\lambda_n R_2)]}{\pi \lambda_n^2 J_0(\lambda_n R_1)}$$

$$\int_{R_1}^{R_2} r \ln(r / R_1) U_0(\lambda_n r) dr = \frac{2[J_0(\lambda_n R_1)] \ln(R_2 / R_1)}{\pi \lambda_n^2 J_0(\lambda_n R_1)}$$

Hence;

$$\int_{R_1}^{R_2} r f(r) U_0(\lambda_n r) dr = \frac{2 [Y_0(\lambda_n R_2)] [-J_0(\lambda_n R_2)]}{\pi \lambda_n^2 J_0(\lambda_n R_1)} \quad (21)$$

Substitute eq. (20) and (21) into eq. (19), and rearranging yields;

$$c_n = \frac{\pi [Y_0(\lambda_n R_2)] [-J_0(\lambda_n R_2)] [J_0(\lambda_n R_1)]}{[J_0^2(\lambda_n R_1) - J_0^2(\lambda_n R_2)]} \quad (22)$$

Substitute eq. (22) into eq. (14), and rearranging yields;

$$\theta(r, t) = \left[\frac{\ln(r / R_1)}{\ln(R_2 / R_1)} \right] - \sum_{n=1}^{\infty} \frac{\pi [J_0(\lambda_n R_2)] [J_0(\lambda_n R_1)]}{[J_0^2(\lambda_n R_1) - J_0^2(\lambda_n R_2)]} U_0(\lambda_n r) e^{-\lambda_n^2 \alpha_m t} \quad (23)$$

Substitute eq. (4) into (6), and rearranging yields;

$$\theta(r, t) = \frac{\int_0^T k(T) dT - \int_0^{T_o} k(T) dT}{\int_{T_o}^{T_i} k(T) dT} \quad (24)$$

Hence, equate eq. (23) and eq. (24) leads to the general analytical close form solution, and it is given as follows;

$$\frac{\int_0^T k(T) dT - \int_0^{T_o} k(T) dT}{\int_{T_o}^{T_i} k(T) dT} = \left[\frac{\ln(r / R_1)}{\ln(R_2 / R_1)} \right] - \sum_{n=1}^{\infty} \frac{\pi [J_0(\lambda_n R_2)] [J_0(\lambda_n R_1)]}{[J_0^2(\lambda_n R_1) - J_0^2(\lambda_n R_2)]} U_0(\lambda_n r) e^{-\lambda_n^2 \alpha_m t} \quad (25)$$

To normalize eq. (25), assume the following:

$$\left. \begin{aligned} \xi &= \frac{R_2}{R_1} \\ r^* &= \frac{r}{R_1} \\ Fo &= \frac{\alpha_m t}{R_1^2} \\ \lambda_n^* &= \lambda_n R_1 \end{aligned} \right\} \quad (26)$$

Therefore:-

$$U_0(\lambda_n^* r^*) = J_0(\lambda_n^* r^*) Y_0(\lambda_n^* \xi) - J_0(\lambda_n^* \xi) Y_0(\lambda_n^* r^*) \quad (27)$$

Hence, substituting eq. (26) into eq. (25) and rearranging, yields the general analytical close form solution of unsteady temperature distribution through the cylindrical thermal insulation material, as follows:

$$T^* = \frac{\int_0^T k(T) dT - \int_0^{T_o} k(T) dT}{\int_{T_o}^{T_i} k(T) dT} = \left[\frac{\ln(r^*)}{\ln(\xi)} \right] - \sum_{n=1}^{\infty} \frac{\pi [J_0(\lambda_n^* \xi)] [J_0(\lambda_n^*)]}{[J_0^2(\lambda_n^*) - J_0^2(\lambda_n^* \xi)]} U_0(\lambda_n^* r^*) e^{-(\lambda_n^*)^2 Fo} \quad (28)$$

The unsteady heat transfer through the cylindrical thermal insulation material is given as follows:-

$$q(r, t) = - \left(-k(T) A_{(r)} \frac{\partial T(r, t)}{\partial r} \right) \quad (29)$$



$$A_{(r)} = 2 \pi rL \tag{30}$$

Differentiating eq. (25) and rearranging, yields:

$$\frac{\partial T(r,t)}{\partial r} = \left[\frac{\int_{T_o}^{T_i} k(T) dT}{k(T)} \cdot \left[\frac{1}{r} \right] \right] \left[\frac{1}{\ln(R_2/R_1)} - \sum_{n=1}^{\infty} \frac{\pi(\lambda_n r) [J_0(\lambda_n R_2)] [J_0(\lambda_n R_1)]}{[J_0^2(\lambda_n R_1) - J_0^2(\lambda_n R_2)]} U_1(\lambda_n r) e^{-\lambda_n^2 \alpha_m t} \right] \tag{31}$$

Where:

$$U_1(\lambda_n r) = Y_1(\lambda_n r) J_0(\lambda_n R_2) - J_1(\lambda_n r) Y_0(\lambda_n R_2)$$

Substituting eq. (30) and eq. (31) into (29), yields:-

$$\frac{q(r,t)}{L} = 2 \pi \left[\int_{T_o}^{T_i} k(T) dT \right] \left[\frac{1}{\ln(R_2/R_1)} - \sum_{n=1}^{\infty} \frac{\pi(\lambda_n r) [J_0(\lambda_n R_2)] [J_0(\lambda_n R_1)]}{[J_0^2(\lambda_n R_1) - J_0^2(\lambda_n R_2)]} U_1(\lambda_n r) e^{-\lambda_n^2 \alpha_m t} \right] \tag{32}$$

To normalize eq. (32), substitute eq. (26) into eq. (32) and rearranging, yields:-

$$\frac{q}{L} = 2 \pi \left[\int_{T_o}^{T_i} k(T) dT \right] \left[\frac{1}{\ln(\xi)} - \sum_{n=1}^{\infty} \frac{\pi(\lambda_n^* r^*) [J_0(\lambda_n^* \xi)] [J_0(\lambda_n^*)]}{[J_0^2(\lambda_n^*) - J_0^2(\lambda_n^* \xi)]} U_1^*(\lambda_n^* r^*) e^{-(\lambda_n^*)^2 Fo} \right] \tag{33}$$

Where:

$$U_1^*(\lambda_n^* r^*) = Y_1(\lambda_n^* r^*) J_0(\lambda_n^* \xi) - J_1(\lambda_n^* r^*) Y_0(\lambda_n^* \xi)$$

And the heat transfer at the inner surface of the thermal insulation material ($r^* = 1$) is given as:

$$\frac{q_o}{L} = 2 \pi \left[\int_{T_o}^{T_i} k(T) dT \right] \left[\frac{1}{\ln(\xi)} - \sum_{n=1}^{\infty} \frac{\pi(\lambda_n^*) [J_0(\lambda_n^* \xi)] [J_0(\lambda_n^*)]}{[J_0^2(\lambda_n^*) - J_0^2(\lambda_n^* \xi)]} U_1^*(\lambda_n^*) e^{-(\lambda_n^*)^2 Fo} \right] \tag{34}$$

$$U_1^*(\lambda_n^*) = Y_1(\lambda_n^*) J_0(\lambda_n^* \xi) - J_1(\lambda_n^*) Y_0(\lambda_n^* \xi)$$

The general analytical close form solution of unsteady heat transfer through the cylindrical thermal insulation material is given as follows:

$$\frac{q}{q_o} = \left[\frac{1}{\ln(\xi)} - \sum_{n=1}^{\infty} \frac{\pi(\lambda_n^* r^*) [J_0(\lambda_n^* \xi)] [J_0(\lambda_n^*)]}{[J_0^2(\lambda_n^*) - J_0^2(\lambda_n^* \xi)]} U_1^*(\lambda_n^* r^*) e^{-(\lambda_n^*)^2 Fo} \right] \left[\frac{1}{\ln(\xi)} - \sum_{n=1}^{\infty} \frac{\pi(\lambda_n^*) [J_0(\lambda_n^* \xi)] [J_0(\lambda_n^*)]}{[J_0^2(\lambda_n^*) - J_0^2(\lambda_n^* \xi)]} U_1^*(\lambda_n^*) e^{-(\lambda_n^*)^2 Fo} \right] \tag{35}$$

3.1 Case study (1): $k(T) = k_m$

3.1.1 Temperature profile:

Substitute the value of (k_m) into eq. (28) and rearranging, yields;

$$\frac{T - T_o}{T_i - T_o} = \left[\frac{\ln(r^*)}{\ln(\xi)} \right] - \sum_{n=1}^{\infty} \frac{\pi [J_0(\lambda_n^* \xi)] [J_0(\lambda_n^*)]}{[J_0^2(\lambda_n^*) - J_0^2(\lambda_n^* \xi)]} U_0(\lambda_n^* r^*) e^{-(\lambda_n^*)^2 Fo}$$

3.1.2 Heat transfer:

Substitute the value of (k_m) into eq. (33) and rearranging, yields;

$$\frac{q}{L} = 2\pi k_m (T_i - T_o) \left[\frac{1}{\ln(\xi)} - \sum_{n=1}^{\infty} \frac{\pi(\lambda_n^* r^*) [J_0(\lambda_n^* \xi)] [J_0(\lambda_n^*)]}{[J_0^2(\lambda_n^*) - J_0^2(\lambda_n^* \xi)]} U_1^*(\lambda_n^* r^*) e^{-(\lambda_n^*)^2 Fo} \right]$$

3.2 Case study (2): $k(T) = a + bT^c$

3.2.1 Temperature profile:

Substitute the temperature dependent thermal conductivity that is proposed by an available empirical function $(k(T) = a + bT^c)$, (Hoffman, 2006) into eq. (28) and rearranging, yields;

$$\frac{\left[aT + \frac{b}{c+1} T^{c+1} \right] - \left[aT_o + \frac{b}{c+1} T_o^{c+1} \right]}{\left[aT_i + \frac{b}{c+1} T_i^{c+1} \right] - \left[aT_o + \frac{b}{c+1} T_o^{c+1} \right]} = \delta \quad (36)$$

Where:

$$\delta = \left[\frac{\ln(r^*)}{\ln(\xi)} \right] - \sum_{n=1}^{\infty} \frac{\pi [J_0(\lambda_n^* \xi)] [J_0(\lambda_n^*)]}{[J_0^2(\lambda_n^*) - J_0^2(\lambda_n^* \xi)]} U_0(\lambda_n^* r^*) e^{-(\lambda_n^*)^2 Fo}$$

To solve eq. (36), assume the following:-

$$g(T) = aT + \frac{b}{c+1} T^{c+1}$$

$$f = [g(T) - g(T_o)] - \delta [g(T_i) - g(T_o)] \quad (37)$$

The root T of eq. (37) is found using the approximate numerical iterative Newton Method, (Gerald, 1989);

$$f' = \frac{df}{dT} = \frac{dg(T)}{dT} = k(T)$$

$$T_{new} = T_{old} - \frac{f_{old}}{f'_{old}}$$

$$T_{new} = T_{old} - \frac{[g(T_{old}) - g(T_o)] - \delta [g(T_i) - g(T_o)]}{k(T_{old})}$$

3.2.2 Heat transfer:

Substitute the value of $(k(T) = a + bT^c)$ into eq. (33) and rearranging, yields;

$$\frac{q}{L} = 2\pi [g(T_i) - g(T_o)] \left[\frac{1}{\ln(\xi)} - \sum_{n=1}^{\infty} \frac{\pi(\lambda_n^* r^*) [J_0(\lambda_n^* \xi)] [J_0(\lambda_n^*)]}{[J_0^2(\lambda_n^*) - J_0^2(\lambda_n^* \xi)]} U_1^*(\lambda_n^* r^*) e^{-(\lambda_n^*)^2 Fo} \right]$$

4. THERMAL CONDUCTIVITY

The dependence of thermal conductivity on temperature is suggested by the empirical function $(k = a + bT^c)$, (Hoffman, 2006). The values of (a, b, c) for the four selected thermal insulation materials are given in **Table 1**. This empirical function is valid in a temperature rang of $(77 - 400 K)$. The thermal conductivity of the first insulation material, Perlite in air at $(10^5 Pa)$ atmospheric pressure, is linearly dependent on temperature, (Perlite Institute Thermal Data Sheet, 1970). In the literatures (Christiansen and Hollingworth, 1958) and (Christiansen, Hollingworth and Marsh, 1959), measurements of the thermal conductivity of micro fine Fiberglass mats are published. This material consists of fibers type ‘AA’ of Owens-Corning Fiberglass Corporation. The behavior of the thermal conductivity and its mean value for each of these thermal insulating materials for a temperature range of $(77 - 300 K)$ is shown in **Fig. 3**.

5. SPECIFIC HEAT CAPACITY

Each of the four selected thermal insulation materials is originally made from Quartz glass. Therefore, the temperature dependence of specific heat capacity of Quartz

glass for a temperature range of $(77 - 300 K)$ is given in **Table 2**, (Corruccini and Gniewek, 1960). In order to evaluate the mean value of specific heat capacity (C_m) of Quartz glass, its relation with temperature is represented using a 4th Degree polynomial fit as shown in **Table 3** and it is plotted with its mean value in **Fig. 4**.

6. THERMAL DIFFUSIVITY

The behavior of thermal diffusivity and its mean value for each of the four selected thermal insulation materials for a temperature range of $(77 - 300 K)$ is shown in **Fig. 5**.

7. RESULTS

Consider four empty cylindrical storage tanks of liquid nitrogen for instance. Each of these tanks is thermally insulated with a hollow cylindrical super insulating material of outside radius ($R_2 = 1m$) and initially at ($T_i = 300 K$). The first thermal insulation material is Perlite of thickness ($800 mm$) with a characteristic mean particle diameter of ($d_m = 0.5 mm$) and density of ($\rho = 64 kg / m^3$) at ($10^5 Pa$) atmospheric pressure. The second is Perlite of thickness ($600 mm$) with a characteristic mean particle diameter of ($d_m = 0.5 mm$) and density of ($\rho = 50 kg / m^3$) at a gas pressure ($\leq 0.1 Pa$). The third is Microglass spheres of thickness ($400 mm$) with a characteristic mean particle diameter of ($d_m = 0.1 mm$) and density of ($\rho = 225 kg / m^3$) at a gas pressure ($\leq 1 Pa$). The fourth is micro fine Fiberglass mats of thickness ($200 mm$) with a mean fiber diameter of ($d_m = 1.143 \mu m$) and density of ($\rho = 240 kg / m^3$) at a gas pressure ($\leq 1 Pa$). The thermal conductivity of the four selected thermal insulation materials is temperature dependent and is proposed by an available empirical function ($k = a + bT^c$), (Hoffman, 2006). The values of (a, b, c) are given in **Table 1**. Then, each of these tanks is suddenly filled with saturated liquid nitrogen at ($T_o = 77 K$). Therefore, each of the four

selected thermal insulation materials is subjected at ($r = R_1$) with a constant temperature of ($T_o = 77 K$).

To plot the transient temperature distribution and the rate of heat transfer of the insulating material, it is necessary to estimate the roots (λ_n^*). The values of these roots are given in **Table 4**, (Cole et. al., 2011).

Figure 6 shows the profiles of temperature distribution for each of the four selected thermal insulation materials for two case studies. The first considers a constant mean value of thermal conductivity (k_m) for the temperature range $(77 - 300 K)$. The general analytical close form solution of the first case study is identical to the solution of (Carslaw and Jaeger, 1959) using the same assumptions. Therefore, the validation of the analytical solution is accomplished perfectly. The second case study is for a temperature dependent thermal conductivity proposed by an available empirical function ($k = a + bT^c$), (Hoffman, 2006). Each profile of the second case study was converged after a maximum of 5 iterations for a temperature residual value of ($1 \times 10^{-6} C^o$). **Table 5** shows the summary of the present work analytical solutions for both case studies.

Figure 7 shows the heat transfer profiles for each of the four selected thermal insulation materials. It is clear that the thermal insulation material that has the lowest value of thermal conductivity has the lowest heat transfer value. **Table 5** shows the summary of the present work analytical solutions.

For both **Figures 6 and 7**, it is clear that the characteristics of the thermal insulation material and the pressure value between its particles have a major effect on the rate of heat transfer and consequently the temperature profile. For instance, the dominant heat transfer mode when choosing Perlite at ($10^5 Pa$) atmospheric pressure is by heat conduction of the interstitial gas between the particles, whereas the heat transfer by radiation is negligible. When the pressure within a thermal insulation material is lowered to a value, the

percentage of heat transfer by heat conduction of the interstitial gas between the particles becomes negligibly small when compared with the percentage heat transfer by radiation and conduction over the bulk material. The gas pressure, at which this is reached, depends on the characteristic diameter of the thermal insulation material. For Perlite with a characteristic mean particle diameter of ($d_m = 0.5\text{ mm}$), a gas pressure of ($\leq 0.1\text{ Pa}$) is sufficient, for Microglass spheres with a characteristic mean particle diameter of ($d_m = 0.1\text{ mm}$) and for micro fine Fiberglass with a mean fiber diameter of ($d_m = 1.143\text{ }\mu\text{m}$), it is ($\leq 1\text{ Pa}$) respectively.

Figures 8 and 9 shows the time history of temperature profiles and rate of heat transfer for each of the four selected thermal insulation materials for a temperature dependent thermal conductivity proposed by an available empirical function ($k = a + bT^c$), (Hoffman, 2006).

The general analytical solution for the history of temperature profiles and heat transfer rates of any size and type of thermal insulation material that is subjected to the assumptions that are listed in article (3) is given in **Table 5** and is plotted in **Figures 10 and 11** respectively.

8. CONCLUSIONS

It is found that the characteristics of the thermal insulation material and the pressure value between its particles have a major effect on the rate of heat transfer and temperature profile. The dominant mode of heat transfer when choosing a specific thermal insulation material at atmospheric pressure is by heat conduction of the interstitial gas between its particles, whereas the heat transfer by radiation is negligible. When the pressure within a thermal insulation material is lowered to a vacuum level, the percentage of heat transfer by heat conduction of the interstitial gas between its particles becomes negligibly small when compared with the percentage heat transfer by radiation and conduction over the bulk material. On the other hand, the optimum selection of thermal insulating material for a

specific cylindrical storage tank of liquefied cryogenic fluid is that with a minimum heat leakage (minimum boil off rate of cryogenic fluid), a minimum amount of insulating material (minimum cost) and a maximum storage capacity of the storage tank (minimum thickness of the thermal insulating material). This optimum selection is accomplished when choosing the micro fine Fiberglass mats when compared with the three other thermal insulating materials.

ACKNOWLEDGEMENTS

The author would like to thank Mr. Hofmann A., "A formerly Linde AG, Geschäftsbereich LE, Germany", for his valuable technical details during email communications. Without his contribution, this paper could not be done.

REFERENCES

- Amiri D.A., Kayhani M.H., Norouzi M., *Exact analytical solution of unsteady axis-symmetric conductive heat transfer in cylindrical orthotropic composite laminates*, International journal of heat and mass transfer, ELSEVIER, 55, 4427-4436, 2012.
- Arpaci V.S., *Conduction heat transfer*, Addison-Wesley, 1966.
- Carslaw H.S. and Jaeger J.C., *Conduction of Heat in Solids*, 2nd ed., Oxford University Press, New York, 1959.
- Christiansen R.M. and Hollingworth Jr.M., *The performance of glass fiber insulation under high vacuum*, Adv. Cryogen Eng., 1958(4):S141.
- Christiansen R.M., Hollingworth Jr.M. and Marsh Jr.H.N., *Low temperature insulation systems*, Adv. Cryogen Eng., 1959(5).
- Cole KD, Haji-Sheikh A, Beck JV, Litkouhi B, *Heat Conduction Using Green's Functions*, 2nd ed., CRC Press, Taylor and Francis Group, 2011.



Corruccini R.J. and Gniewek J.J., *Specific Heats and Enthalpies of Technical Solids at Low Temperatures*, NBS Monograph, 21, 1960.

Gerald C.F. and Wheatley P.O., *Applied Numerical Analysis*, 4th ed., Addison-Wesley, New York, 1989.

Hofmann A., *The thermal conductivity of cryogenic insulation materials and its temperature dependence*, Elsevier, Cryogenics, 46, 815-824, 2006.

Kaganer, *Thermal Insulation in Cryogenic Engineering*, Israel Program for Scientific Translations, 1969.

Kropschot R.H. and Burges R.W., *Perlite for cryogenic insulation*, Adv. Cryogen Eng., 1962(8):S425.

Perlite Institute New York, *Thermal Data Sheet No. 2-4*, 1970.

Singh S., Jain P.K., Rizwan-Uddin, *Analytical solution to transient heat conduction in polar coordinates with multiple layers in radial direction*, International journal of thermal sciences, ELSEVIER, 47, 261-273, 2008.

Verschoor and Greebler, *Heat transfer by gas conduction and radiation in fibrous insulations*, Transactions of ASME Paper No. 51-A54, 1952.

Zivkovic M.M., Nikolic A.V., Slavkovic R.B. and Zivic F.T., *Non-Linear transient heat conduction analysis of insulation wall of tank for transportation of liquid Aluminum*, Thermal Science, Vol. 14, Suppl., S299-S312, 2010.

NOMENCLATURE

- a Constant
- A Cross section area, m²
- b Constant
- c Constant
- C Specific heat Capacity, kJ/kg.K
- d Particle diameter, mm
- Fo Fourier Number

- J₀, J₁ Ordinary Bessel functions of the 1st kind, zero and 1st order respectively
- k Thermal conductivity, W/m.K
- L Length, m
- q Rate of heat transfer, W
- r Distance along the r-direction, m
- R₁ Inner radius, m
- R₂ Outer radius, m
- T Temperature, K
- t Time, second
- Y₀, Y₁ Ordinary Bessel function of the 2nd kind, zero and 1st order respectively

GREEK SYMBOLS

- α Thermal diffusivity, m²/s
- δ Dimensionless parameter
- λ_n Root values of equation (15), m⁻¹
- μ Area under the Kirchhoff's transformation curve, W/m
- θ Dimensionless parameter
- ρ Density, kg/m³
- σ Dimensionless parameter
- Ω Area under the Kirchhoff's transformation curve, W/m
- ξ Ratio of outer to inner radius
- ψ Area under the Kirchhoff's transformation curve, W/m

SUBSCRIPTS

- i Initial
- m Mean
- o Inner surface

SUPERSCRIPTS

- * Dimensionless sign
- ** Arbitrary

Table 1 Suggested empirical function and constant values for the selected thermal insulation materials, (Hoffman, 2006).

Insulating material	Empirical function $(k = a + bT^c)$, $(W/m.K)$		
	<i>a</i>	<i>b</i>	<i>c</i>
Perlite in air $\rho = 64 \text{ kg/m}^3, d_m = 0.5 \text{ mm}, p = 10^5 \text{ Pa}$	8.25×10^{-3}	1.165×10^{-4}	1.0
Perlite - vacuum $\rho = 50 \text{ kg/m}^3, d_m = 0.5 \text{ mm}, p \leq 0.1 \text{ Pa}$	1.9112×10^{-4}	3.4757×10^{-12}	3.678
Microglass spheres – vacuum $\rho = 225 \text{ kg/m}^3, d_m = 0.1 \text{ mm}, p \leq 1 \text{ Pa}$	3.7037×10^{-4}	7.4041×10^{-11}	3.0158
Fiberglass – vacuum $\rho = 240 \text{ kg/m}^3, d_m = 1.143 \mu\text{m}, p \leq 1 \text{ Pa}$	2.7074×10^{-4}	3.083×10^{-11}	3.0

Table 2 Data values of specific heat capacity for Quartz glass with temperature, (Corruccini and Gniewek, 1960).

T (K)	50	100	150	200	250	300
C (J/g.K)	0.095	0.21	0.41	0.54	0.65	0.745

Table 3 Data values for a 4th Degree polynomial fit of specific heat capacity for Quartz glass with temperature.

$C(T) = \sum_{n=0}^4 \beta_n T^n$, $(J/kg.K)$				
β_0	β_1	β_2	β_3	β_4
2.16667×10^2	- 6.485582	9.92778×10^{-2}	$- 3.9926 \times 10^{-4}$	5.333×10^{-7}

Table 4 First Five Roots of : $J_0(\lambda^*)Y_0(\lambda^*\xi) - Y_0(\lambda^*)J_0(\lambda^*\xi)$, (Where $\xi = R_2/R_1$, $\xi > 1$), (Cole et. al., 2011).

ξ^{-1}	λ_1^*	λ_2^*	λ_3^*	λ_4^*	λ_5^*
0.80	12.55847031	25.12877	37.69646	50.26349	62.83026
0.60	4.69706410	9.41690	14.13189	18.84558	23.55876
0.40	2.07322886	4.17730	6.27537	8.37167	10.46723
0.20	0.76319127	1.55710	2.34641	3.13403	3.92084
0.10	0.33139387	0.68576	1.03774	1.38864	1.73896
0.08	0.25732649	0.53485	0.81055	1.08536	1.35969
0.06	0.18699458	0.39079	0.59334	0.79522	0.99673
0.04	0.12038637	0.25340	0.38570	0.51759	0.64923
0.02	0.05768450	0.12272	0.18751	0.25214	0.31666
0.00	0.00000000	0.00000	0.00000	0.00000	0.00000



Table 5 Summary of analytical solutions.

Case study	Thermal conductivity [W / m.K]	Temperature profile T, [K]	Heat transfer q, [W]
0	$k(T)$	$T^* = \frac{\int_0^T k(T)dT - \int_0^{T_o} k(T)dT}{\int_{T_o}^{T_i} k(T)dT} =$ $\left[\frac{\ln(r^*)}{\ln(\xi)} \right] - \sum_{n=1}^{\infty} \frac{\pi [J_0(\lambda_n^* \xi)] [J_0(\lambda_n^*)]}{[J_0^2(\lambda_n^*) - J_0^2(\lambda_n^* \xi)]} U_0(\lambda_n^* r^*) e^{-(\lambda_n^*)^2 Fo}$	$\frac{q}{q_o} = \frac{1}{\ln(\xi)} - \sum_{n=1}^{\infty} \frac{\pi (\lambda_n^* r^*) [J_0(\lambda_n^* \xi)] [J_0(\lambda_n^*)]}{[J_0^2(\lambda_n^*) - J_0^2(\lambda_n^* \xi)]} U_1^*(\lambda_n^* r^*) e^{-(\lambda_n^*)^2 Fo}$ $\frac{1}{\ln(\xi)} - \sum_{n=1}^{\infty} \frac{\pi (\lambda_n^*) [J_0(\lambda_n^* \xi)] [J_0(\lambda_n^*)]}{[J_0^2(\lambda_n^*) - J_0^2(\lambda_n^* \xi)]} U_1^*(\lambda_n^*) e^{-(\lambda_n^*)^2 Fo}$
1	$k(T) = k_m$	$\frac{T - T_o}{T_i - T_o} =$ $\left[\frac{\ln(r^*)}{\ln(\xi)} \right] - \sum_{n=1}^{\infty} \frac{\pi [J_0(\lambda_n^* \xi)] [J_0(\lambda_n^*)]}{[J_0^2(\lambda_n^*) - J_0^2(\lambda_n^* \xi)]} U_0(\lambda_n^* r^*) e^{-(\lambda_n^*)^2 Fo}$	$\frac{q}{L} = 2 \pi k_m (T_i - T_o)$ $\left[\frac{1}{\ln(\xi)} - \sum_{n=1}^{\infty} \frac{\pi (\lambda_n^* r^*) [J_0(\lambda_n^* \xi)] [J_0(\lambda_n^*)]}{[J_0^2(\lambda_n^*) - J_0^2(\lambda_n^* \xi)]} U_1^*(\lambda_n^* r^*) e^{-(\lambda_n^*)^2 Fo} \right]$
2	$k(T) = a + bT^c$	$\frac{\left[aT + \frac{b}{c+1} T^{c+1} \right] - \left[aT_o + \frac{b}{c+1} T_o^{c+1} \right]}{\left[aT_i + \frac{b}{c+1} T_i^{c+1} \right] - \left[aT_o + \frac{b}{c+1} T_o^{c+1} \right]} =$ $\left[\frac{\ln(r^*)}{\ln(\xi)} \right] - \sum_{n=1}^{\infty} \frac{\pi [J_0(\lambda_n^* \xi)] [J_0(\lambda_n^*)]}{[J_0^2(\lambda_n^*) - J_0^2(\lambda_n^* \xi)]} U_0(\lambda_n^* r^*) e^{-(\lambda_n^*)^2 Fo}$	$\frac{q}{L} = 2 \pi \left\{ \left[aT_i + \frac{b}{c+1} T_i^{c+1} \right] - \left[aT_o + \frac{b}{c+1} T_o^{c+1} \right] \right\}$ $\left[\frac{1}{\ln(\xi)} - \sum_{n=1}^{\infty} \frac{\pi (\lambda_n^* r^*) [J_0(\lambda_n^* \xi)] [J_0(\lambda_n^*)]}{[J_0^2(\lambda_n^*) - J_0^2(\lambda_n^* \xi)]} U_1^*(\lambda_n^* r^*) e^{-(\lambda_n^*)^2 Fo} \right]$

Where: $\frac{q_o}{L} = 2 \pi \left[\int_{T_o}^{T_i} k(T)dT \right] \left[\frac{1}{\ln(\xi)} - \sum_{n=1}^{\infty} \frac{\pi (\lambda_n^*) [J_0(\lambda_n^* \xi)] [J_0(\lambda_n^*)]}{[J_0^2(\lambda_n^*) - J_0^2(\lambda_n^* \xi)]} U_1^*(\lambda_n^*) e^{-(\lambda_n^*)^2 Fo} \right]$,

$U_o(\lambda_n^* r^*) = J_0(\lambda_n^* r^*) Y_0(\lambda_n^* \xi) - J_0(\lambda_n^* \xi) Y_0(\lambda_n^* r^*)$, $U_1^*(\lambda_n^* r^*) = Y_1(\lambda_n^* r^*) J_0(\lambda_n^* \xi) - J_1(\lambda_n^* r^*) Y_0(\lambda_n^* \xi)$, $U_1^*(\lambda_n^*) = Y_1(\lambda_n^*) J_0(\lambda_n^* \xi) - J_1(\lambda_n^*) Y_0(\lambda_n^* \xi)$
 $\xi = R_2 / R_1$, $r^* = r / R_1$, $Fo = \alpha_m t / R_1^2$, $\lambda_n^* = \lambda_n R_1$

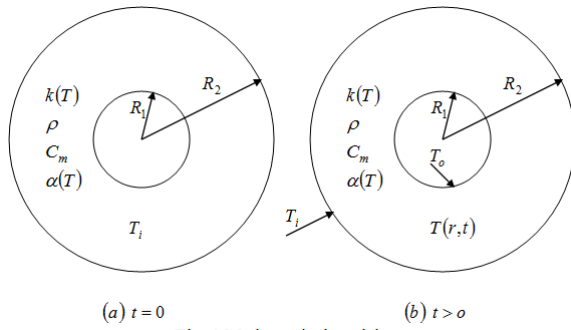


Fig. 1 Mathematical model.

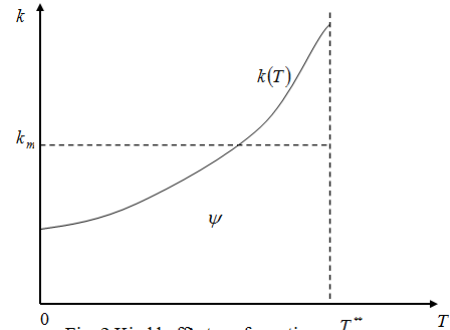


Fig. 2 Kirchhoff's transformation.

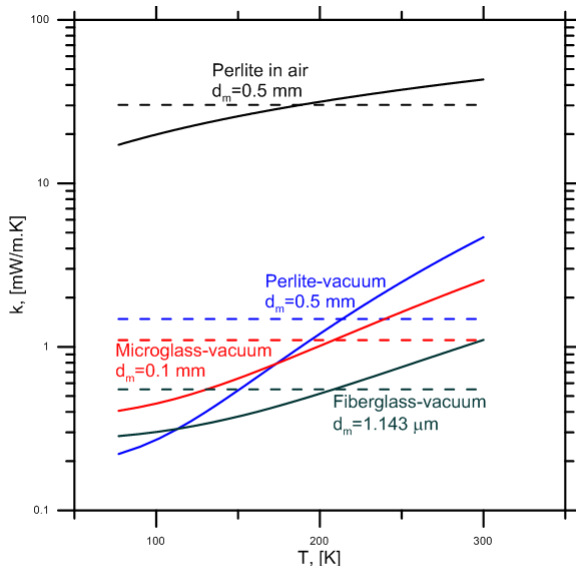


Fig. 3 Thermal conductivity, (Hoffman, 2006)
 (i) Solid lines $k(T)=a+bT^c$
 (ii) Dashed lines $k(T)=k_m$ (77-300 K)

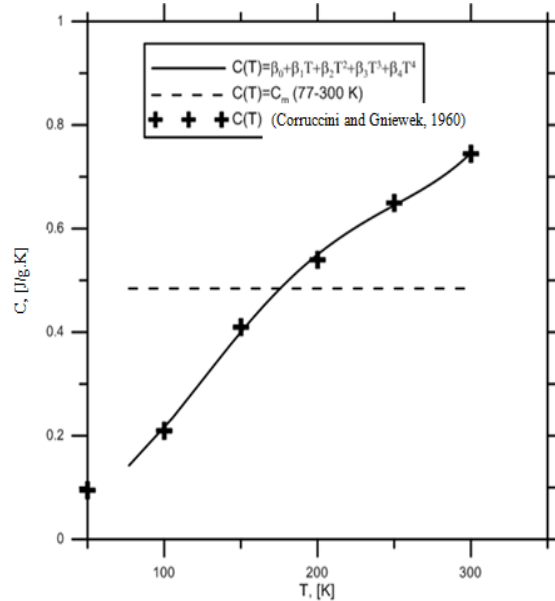


Fig. 4 Specific heat capacity for quartz glass.

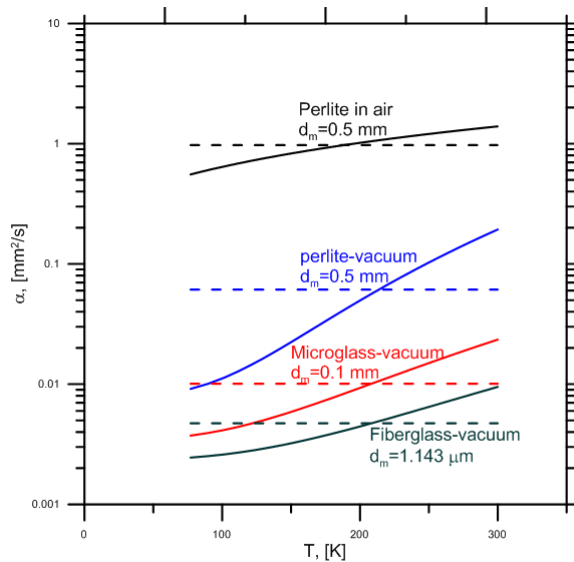


Fig. 5 Thermal diffusivity,
 (i) Solid lines, $\alpha(T)=k(T)/\rho C_m$
 (ii) Dashed lines, $\alpha(T)=\alpha_m$ (77-300 K)

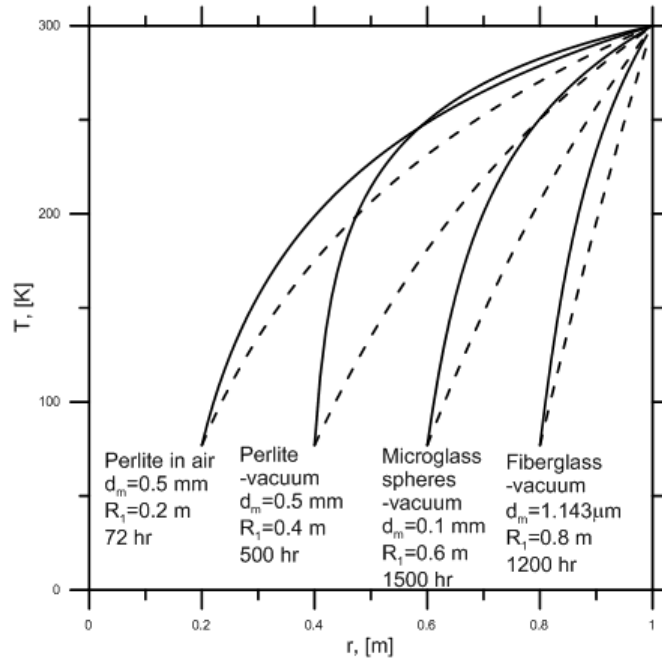


Fig. 6 Temperature profiles.

(i) Solid lines (present work), $k(T)=a+bT^c$

(ii) Dashed lines (present work and (Carslaw and Jaeger, 1959)), $k(T)=k_m(77-300 K)$.

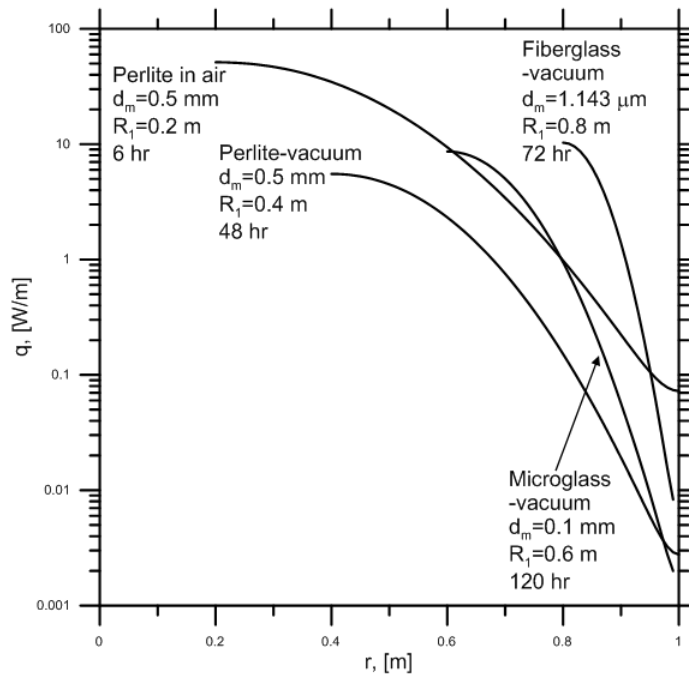
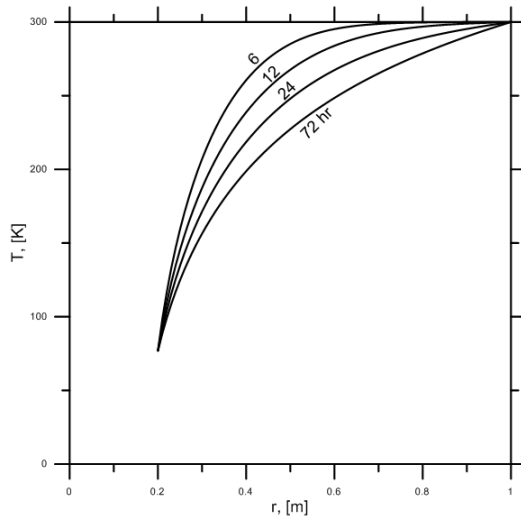
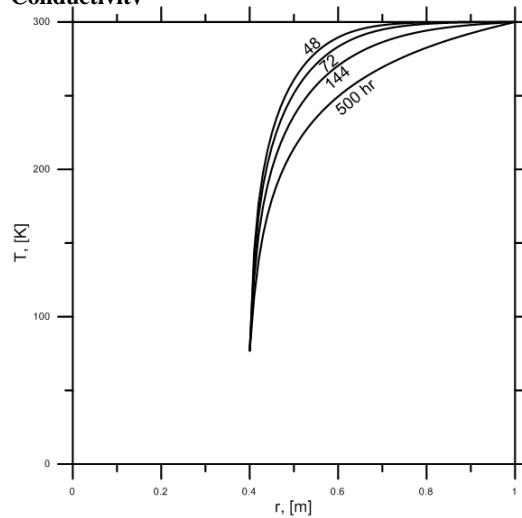


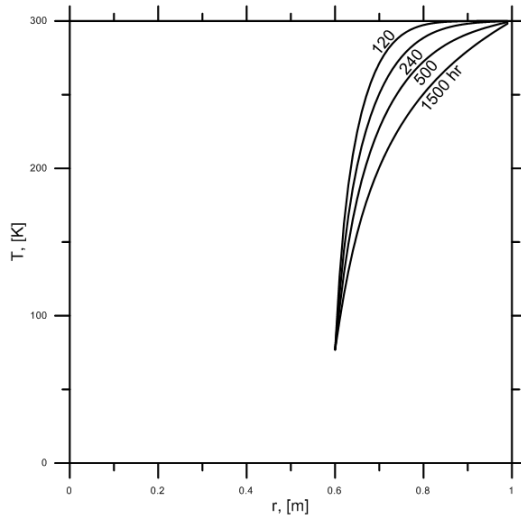
Fig. 7 Heat transfer profiles.



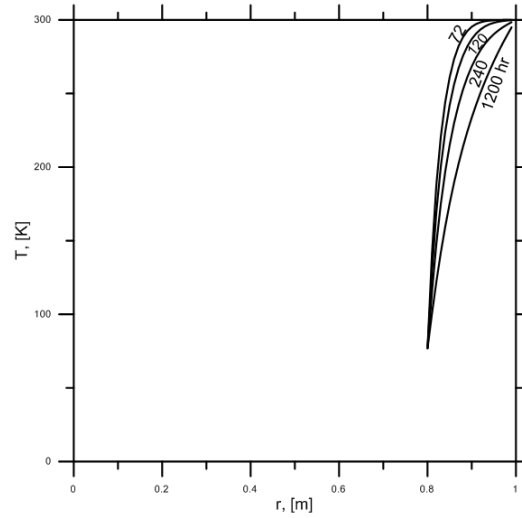
(a) Perlite in air ($d_m=0.5$ mm, $R_i=0.2$ m)



(b) Perlite-vacuum ($d_m=0.5$ mm, $R_i=0.4$ m)



(c) Microglass spheres-vacuum ($d_m=0.1$ mm, $R_i=0.6$ m)



(d) Fiberglass-vacuum ($d_m=1.143$ μ m, $R_i=0.8$ m)

Fig. 8 History of temperature profiles.

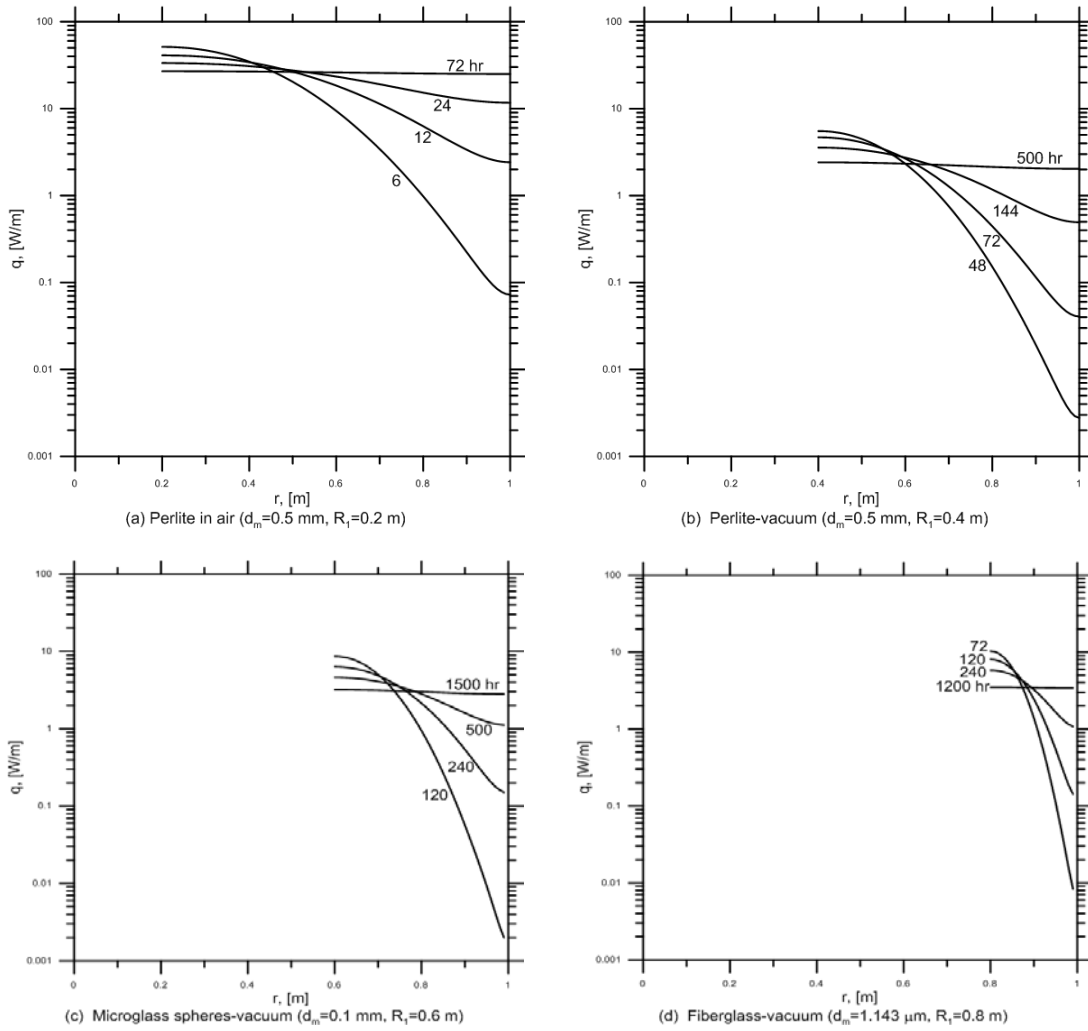
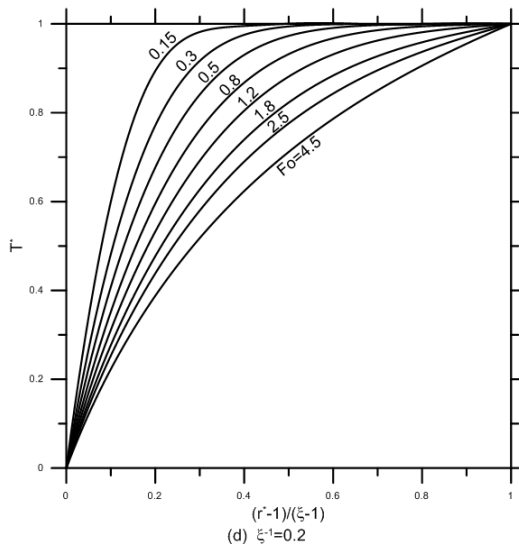
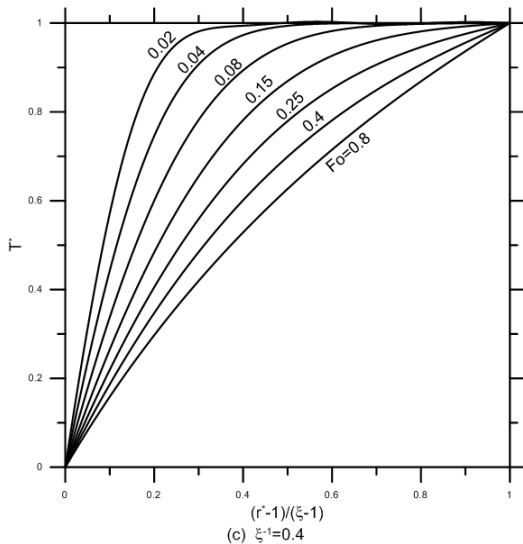
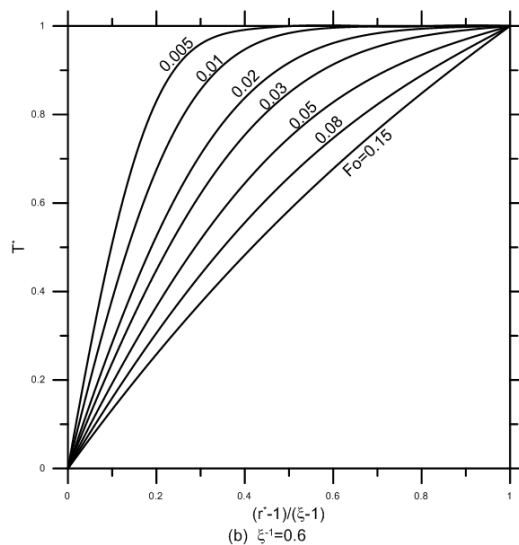
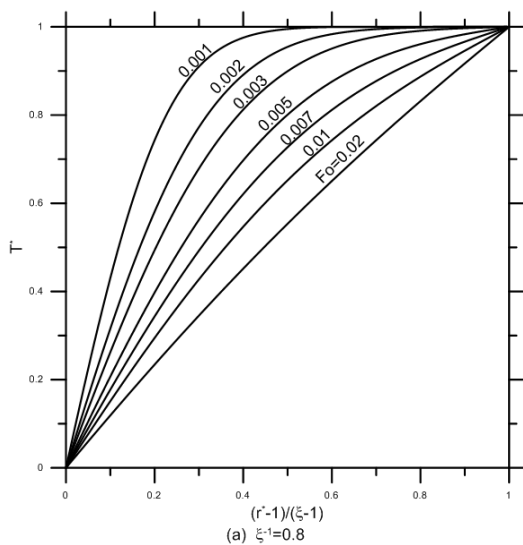


Fig. 9 History of heat transfer profiles.



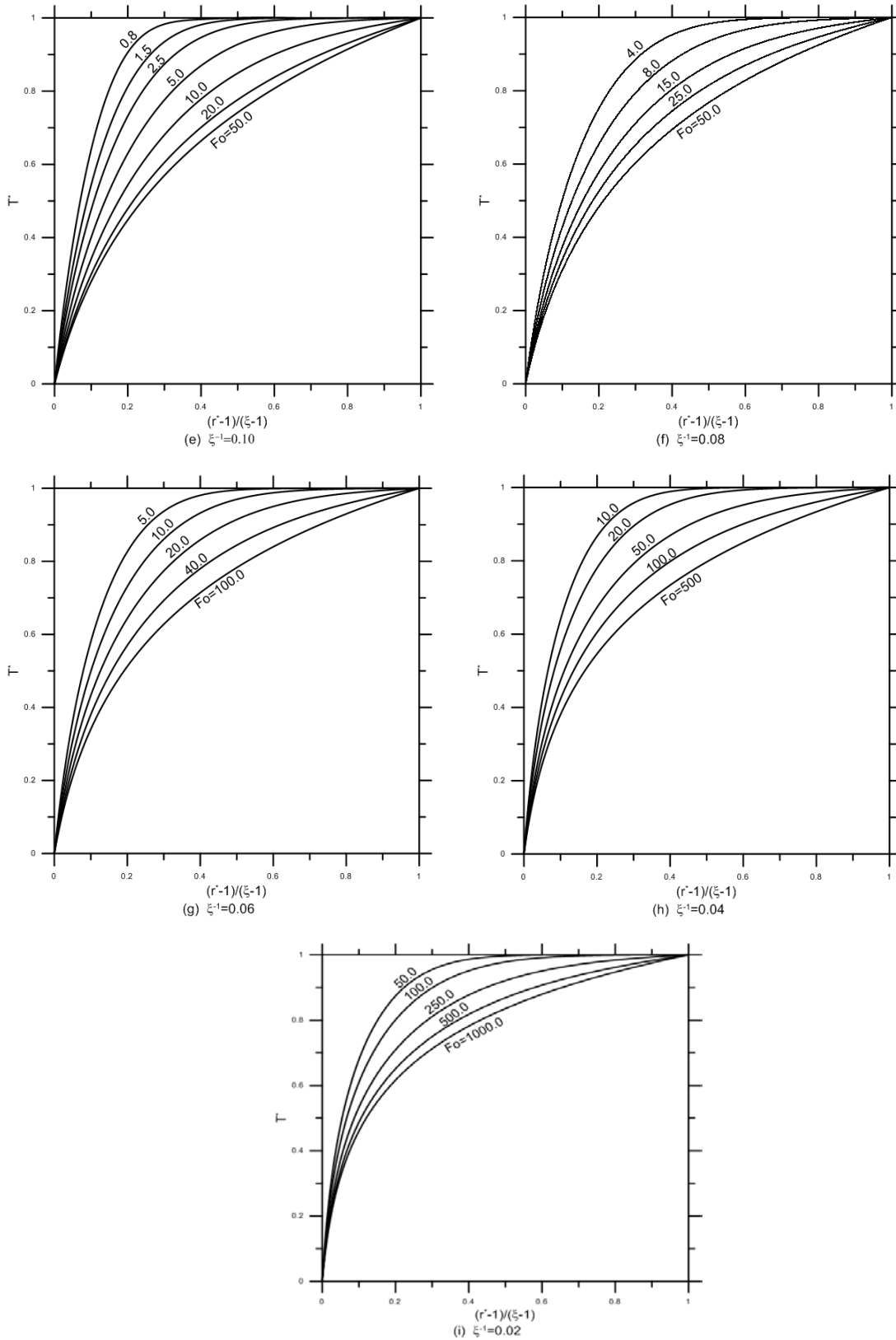
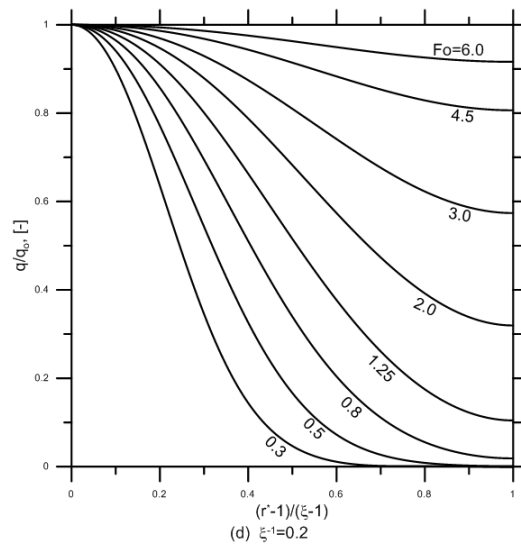
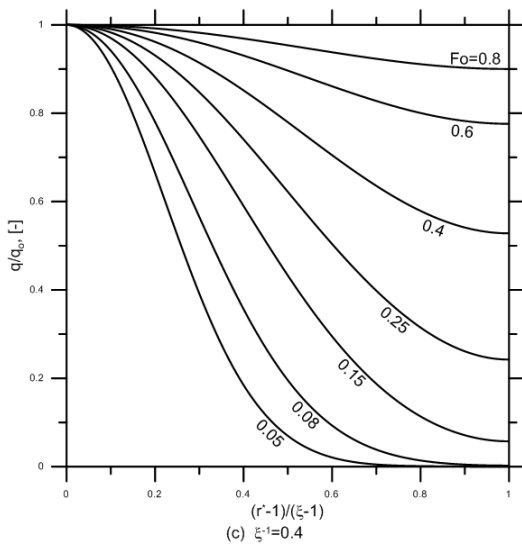
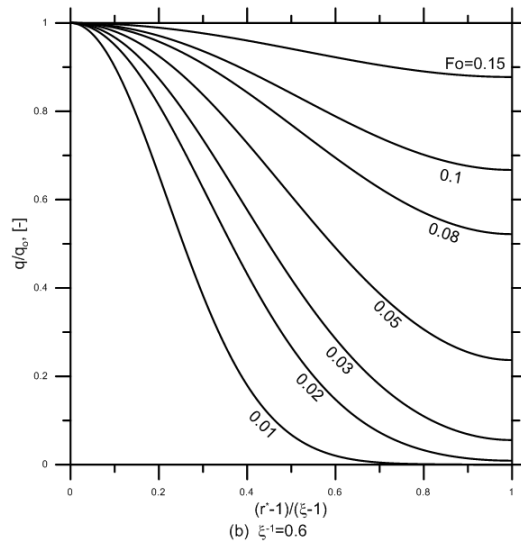
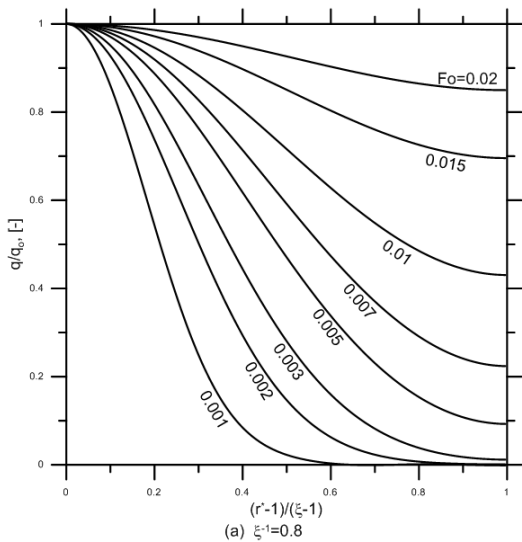


Fig. 10 History of temperature profiles.



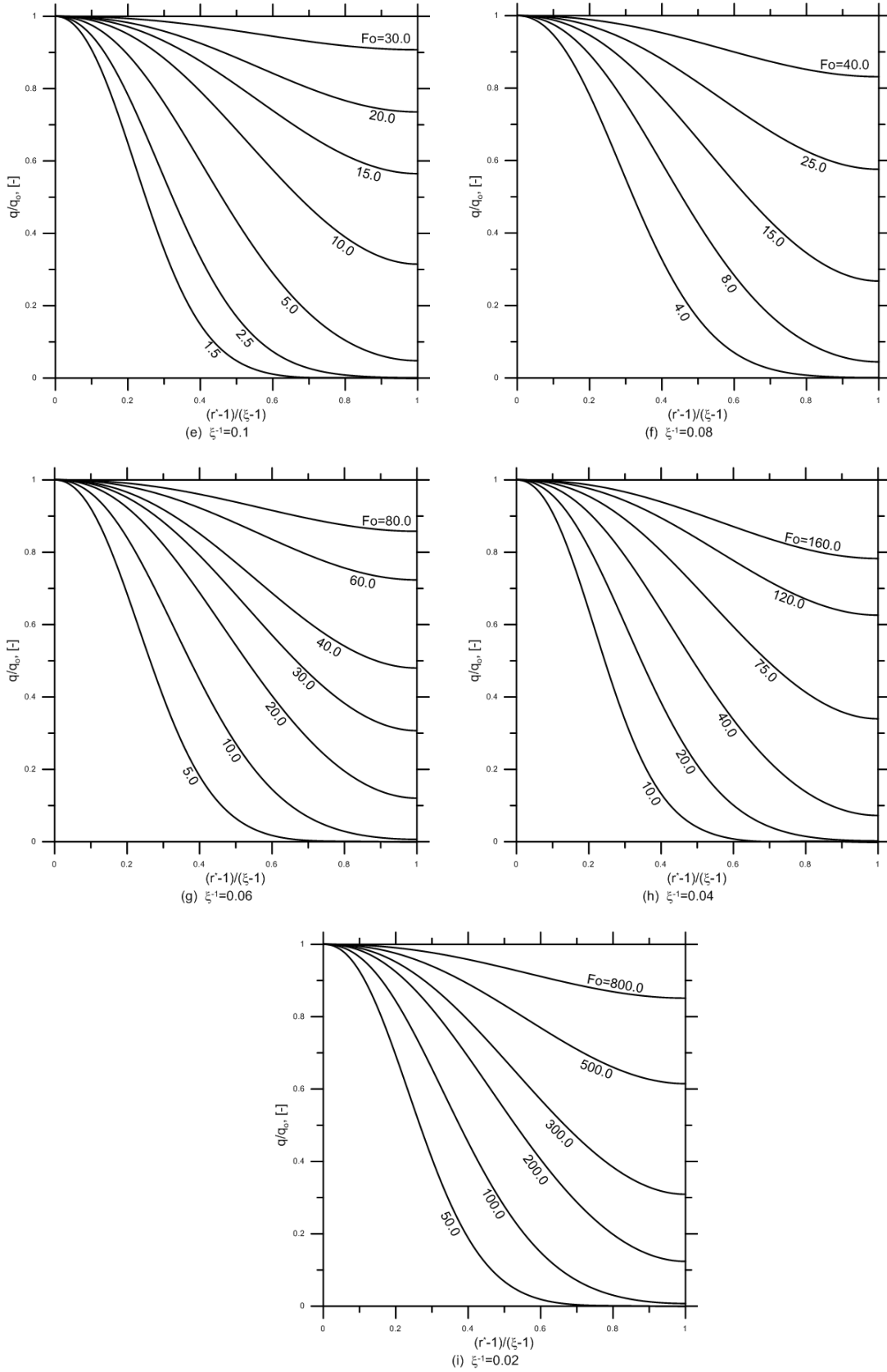


Fig. 11 History of heat transfer profiles.